J Mater Sci (2006) 41:6015–6025
DOI 10.1007/s10853-006-0364-5

Fractographic and numerical study of hydrogen–plasticity interactions near a crack tip

J. Toribio · V. Kharin

Received: 12 May 2003 / Accepted: 18 August 2005 / Published online: 1 August 2006

Abstract This paper offers a fractographic and numerical study of hydrogen–plasticity interactions in the vicinity of a crack tip in a high-strength pearlitic steel subjected to previous cyclic (fatigue) precracking and posterior hydrogen-assisted cracking (HAC) under rising (monotonic) loading conditions. Experiments demonstrate that heavier cyclic preloading improves the HAC behaviour of the steel. Fractographic analysis shows that the microdamage produced by hydrogen is detectable through a specific microscopic topography: tearing topography surface or TTS. A high resolution numerical modelling is performed to reveal the elastoplastic stress–strain field in the vicinity of the crack tip subjected to cyclic preloading and subsequent monotonic loading up to the fracture instant in the HAC tests, and the calculated plastic zone extent is compared with the hydrogen-assisted microdamage region (TTS). Results demonstrate that the TTS depth has no relation with the active plastic zone dimension, i.e., with the size of the only region in which there is dislocation movement, so hydrogen transport cannot be attributed to dislocation dragging, but rather to random-walk lattice diffusion. It is, however, stress-assisted diffusion in which the hydrostatic stress field plays a relevant role. The beneficial effect of crack-tip plastic straining on HAC behaviour might be produced by the delay of hydrogen entry caused by residual compressive stresses and by the enhanced trapping of hydrogen as a consequence of the increase of dislocation density after cyclic plastic straining.

J. Toribio (✉)
Department of Materials Engineering, University of Salamanca, E.P.S., Campus Viriato, Avda Requejo 33, 49022 Zamora, Spain
e-mail: toribio@usal.es

V. Kharin
Pidstryhach Institute for Applied Mechanics and Mathematics, Lviv, Ukraine

Introduction

Hydrogen is known to be a strong promoter of metals failure, so that the study of hydrogen–plasticity interactions is a fundamental issue to clarify the physical micromechanisms leading to hydrogen-assisted fracture of metallic materials. The relationship between hydrogen and plasticity has been the object of many controversial discussions in two opposite senses: (i) whether or not hydrogen influences plasticity by easing dislocations mobility or multiplication and promoting slip band formation or strain localisation; (ii) whether or not plastic zone spreading—and the associated movement of dislocations—can affect hydrogen transport.

Since there is general agreement that hydrogen transport plays a key role in hydrogen-assisted cracking (HAC), it is important to elucidate the *dominant* transport mechanism operative over relevant penetration distances. A great research effort has been made in recent years in this area. The problem, however, is far from being totally understood, and two main modes of hydrogen transport in metals have been proposed: *lattice diffusion* [1–3] (or random-walk diffusion) and *dislocation sweeping* [4–6] (or dislocation dragging). Thus a key question arises as to determine whether the main part of hydrogen transport is carried out by

random-walk lattice diffusion or by dislocation movement, the latter associated with interactions between hydrogen and plasticity.

Diffusion is a transport mode by which hydrogen moves towards the points of minimum saturation of the available sites in the crystalline lattice in the form of random-walk characterised by the $\sqrt{Dt}$ term which estimates the penetration distance depending on the hydrogen diffusion coefficient D and diffusion time t [1]. If stress-assisted diffusion is considered [2], hydrogen movement is driven by the gradients of both concentration and hydrostatic stress since the latter affects the density of available sites to be occupied by hydrogen, and this way influences the degree of metal saturation at a certain amount of absorbed hydrogen. A more general treatment [3] involves also plastic strain as a factor influencing hydrogen solubility, and therefore diffusion, so that stress–strain field gradients contribute to the diffusion driving force. A mechanism of hydrogen transport based on diffusion is consistent with the results of slow strain rate tests in conditions of environmental hydrogenation under cathodic polarisation, since it predicts maximum hydrogen effect at the slowest strain rates [7].

Dislocation sweeping is a transport mode by which hydrogen is dragged by dislocations as the plastic zone spreads. This may be associated with the average velocity of dislocations that can be associated with the plastic strain rate. There are two main models to evaluate the supersaturation or enrichment with hydrogen at specific sites in a material as a result of a dislocation sweep-in of hydrogen: the *stripping model* by Tien et al. [4] and the *annihilation model* by Johnson and Hirth [5], both reviewed in [6]. The first predicts a significant build-up of hydrogen stripped from moving dislocations by a stronger trap, while the latter yields that the kinematic supersaturations of hydrogen left at the sites of dislocation annihilation are extremely small in real situations. The weakest point of the two models is their inconsistency with the well-known experimental evidence of the inverse dependence of hydrogen embrittlement upon strain rate (over a certain range of strain rates). The stripping model predicts maximum hydrogen embrittlement at an intermediate strain rate, whereas according to the annihilation model the kinetic supersaturation is proportional to the strain rate, In addition, the question about the distance along which hydrogen can be effectively dragged by dislocations (a key item in hydrogen-assisted fracture) still remains unresolved.

The two transport modes—diffusional and dislocational—are substantially different. The first one is operative under both sustained and transient stress–strain states, it has instantaneous hydrostatic stress and plastic strain distributions as responsible factors, and evolves towards equilibrium hydrogen saturation (distribution). In contrast, the other one proceeds exclusively during continuing (dynamic) straining, has plastic strain *rate* as the governing variable, and results in non-equilibrium hydrogen distributions (temporal localised over-saturations). These latter are fed by newly arriving dislocations which drive hydrogen into specific microstructural sites, from which hydrogen escapes by lattice diffusion to restore thermodynamic equilibrium with surroundings. Shortly after the end of straining, those hydrogen over-saturations relax to local equilibrium by short-range diffusion. The efficiency of hydrogen accumulation by dislocational transport results from competition between these two in- and out-flows.

The issue of the controlling hydrogen transport mode was addressed in previous research on hydrogen-assisted fracture in *notched* specimens of high-strength pearlitic steel [8, 9] where a detailed analysis of hydrogen-plasticity interactions in the vicinity of notches was provided, showing that stress-assisted diffusion is the predominant mode of transport in pearlitic steel under triaxial stress states produced by notches and that there is no relationship between the plastic zone extent and the hydrogen-affected region revealed by microscopic examination. Thus dislocation transport of hydrogen might not be a critical step for hydrogen embrittlement, and the question of whether or not dislocational transport should be considered as an embrittlement (damaging) mechanism *per se* still remains open.

This paper tries to provide more insight into this fundamental question related to hydrogen–plasticity interactions. The work deals with *precracked* specimens of high-strength pearlitic steel and analyses the mechanical aspects of the effect of fatigue precracking regime on the posterior HAC of the steel. To this end, experiments are considered in combination with a high resolution numerical modelling of the elastoplastic stress–strain field in the vicinity of the crack tip subjected to fatigue precracking and subsequent monotonic loading up to the points of fracture in the HAC tests. Thus, the plastic zone extent is compared with the region affected by the hydrogen at the microscopical level. In addition, since different fatigue precracking programmes are considered, the important effects of prestressing and prestraining in the vicinity of the crack tip can be elucidated. These effects are shown to play an important role in environmentally assisted cracking, especially in the matter of experimental evaluation of

thresholds where the fatigue precracking levels affect dramatically the stress intensity factor for initiation of stress corrosion cracking in general or HAC in particular [10, 11].

Experimental programme

A high strength eutectoid steel was used in this work. The chemical composition is given in Table 1 and the mechanical properties in Table 2. The microstructure of the steel consisted of fine pearlite. To evaluate the HAC behaviour of the steel, slow strain rate tests were performed on transversely precracked rods immersed in aqueous environment under electrochemical control, as described elsewhere [12]. The applied displacement rate was 8.3×10^{-8} ms^{-1}, based on previous experience [13]. The constant electrochemical potential of −1200 mV SCE (cathodic) was held during the tests to create environmental conditions promoting HAC.

Precracking of the samples was carried out by fatigue in the laboratory air environment. Various series of samples were prepared using different zero-to-tension fatigue loads during the last stage of fatigue precracking just previous to the environmentally-assisted fracture test, so as to control this important experimental variable which clearly influences the results in environmentally assisted cracking in general and HAC in particular [12]. The maximum levels of stress intensity factor (K) during the last stage of fatigue were $K_{max} = 0.28K_{IC}$, $0.45K_{IC}$, $0.60K_{IC}$ and $0.80K_{IC}$, where K_{IC} is the fracture toughness of the material in air (cf. Table 2). Therefore, all the parameters affecting the HAC process (specimen geometry, loading mode and rate, hydrogenation conditions) were kept constant, with the exception of the fatigue precracking regime (last stage) whose intensity (K_{max}) was varied from one to another case.

Table 1 Chemical composition (wt %) of the steel

C	Mn	Si	P	S	Cr	Ni	Mo
0.74	0.70	0.20	0.016	0.023	0.01	0.01	0.001

Figure 1 shows the experimental results of the failure load in a hydrogen environment F_{HAC} (divided by the reference value at rupture in air F_C) as a function of the ratio K_{max}/K_{IC}. The mechanical effect of fatigue precracking is beneficial for the HAC resistance of the steel, since the fracture load in hydrogen is an increasing function of K_{max}. This phenomenon may be caused by the development of the cyclic plastic zone and the presence of compressive stresses (cyclic residual stresses) in the vicinity of the crack tip as a consequence of the fatigue precracking procedure. The crack tip is prestrained (and also prestressed) by fatigue: the higher the cyclic load level, the more pronounced is the prestraining/prestressing effect which delays the hydrogen entry and improves material performance.

A fractographic analysis of the samples by scanning electron microscopy was performed after the HAC tests. The most important finding was the presence, between the fatigue precrack and the final fracture by cleavage, of a characteristic region where the microscopic mode of failure is the so called *tearing topography surface* or TTS [14, 15]. Figure 2 shows a scanning electron micrograph of this special topography that resembles microdamage or microtearing. This non-conventional microscopic fracture mode is fundamental in HAC of pearlitic steel because of the strong experimental evidence that allows the consideration of the TTS zone as the hydrogen-assisted microdamage region, i.e., the zone where the physical micromechanisms of hydrogen-assisted fracture operate at the finest microscopical level [16–18] and thus such a zone also represents the subcritical propagation distance under HAC conditions for each level of fatigue precracking (K_{max}).

The depth of the TTS zone was measured in the direction perpendicular to the crack front on the fracture surface (crack plane), in all cases at the deepest point of the crack. Results are given in Fig. 3, showing an inverse relationship between the TTS depth and the maximum stress intensity level during the last stage of fatigue precracking K_{max}, i.e., the

Table 2 Mechanical properties of the steel

Young mod. E (GPa)	Yield stress σ_Y (MPa)	UTS σ_R (MPa)	Fracture/Toughness K_{IC} (MPam$^{1/2}$)	Ramberg–Osgood $\varepsilon = \varepsilon^e + \varepsilon^p = \sigma/E + (\sigma/P)^n$			
				Section I ($\varepsilon^p \le 1.07$)		Section II ($\varepsilon^p > 1.07$)	
				P_I (MPa)	n_I	P_{II} (MPa)	n_{II}
195	725	1300	53	2120	5.8	2160	17

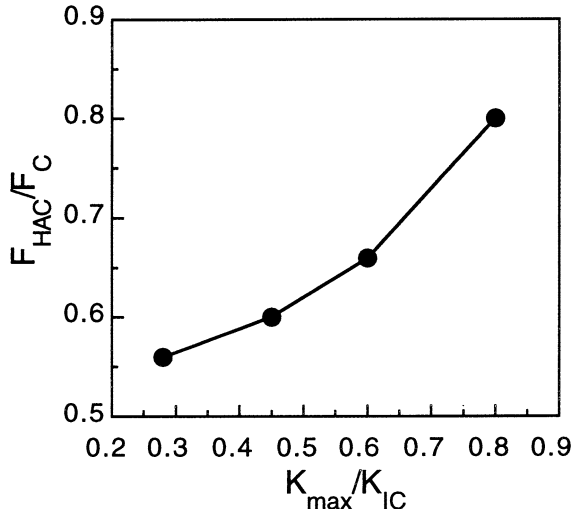

Fig. 1 Results of the rising load HAC tests expressed in terms of the ratio of the failure load in hydrogen F_{HAC} to the same in air F_C as a function of the fatigue precracking level represented by K_{max}/K_{IC}

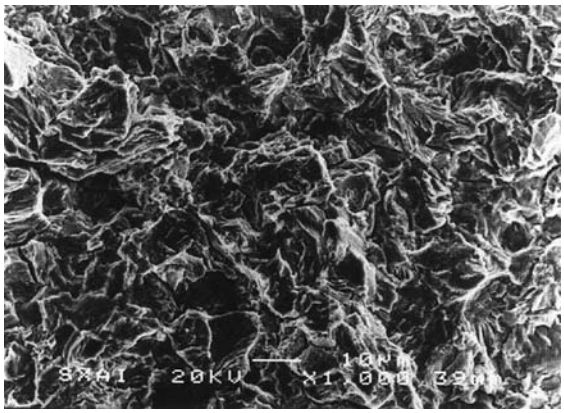

Fig. 2 Microscopic mode of fracture produced by HAC beyond after the fatigue precrack: tearing topography surface (TTS)

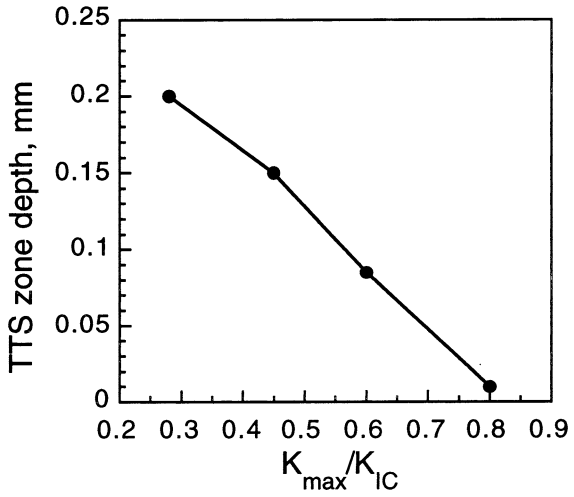

Fig. 3 Depth of the TTS zone in the vicinity of the precrack tip as a function of the fatigue precracking level K_{max}

stronger the fatigue precracking, the narrower the TTS region (the hydrogen damaged domain) in the vicinity of the crack tip, Thus, considering that fatigue precracking, apart from creation of the compressive residual stresses, surely affects the advance of crack tip plasticity in the posterior HAC test, comparison between the scale of the hydrogen-affected zone and the expansion of plasticity is expected to provide insight on hydrogen–plasticity interaction in the steel subjected to HAC.

Numerical modelling

The aim of the modelling is to obtain the evolution of the plastic zone, where dislocation movement goes on, in the rising load HAC test affected by the residual stress–strain state generated by irreversibility of plastic deformations during fatigue precracking. This zone is inaccessible for direct observation, but its characterisation and subsequent comparison with the extents of the hydrogen induced microdamage region is expected to help elucidation of certain aspects of hydrogen–plasticity interactions.

To this end, a numerical simulation was performed of the stress–strain state near the crack tip under plane-strain small-scale yielding in an elastoplastic material with mixed isotropic/kinematic strain-hardening whose characteristics are those of the steel used in the experimental programme (Table 2). According to the theory of plasticity, generalised variables (the equivalent stress σ_{eq} in the von Mises sense and the equivalent strain, ε_{eq}, as well as its elastic and plastic components ε^{e}_{eq} and ε^{p}_{eq} respectively) are employed to represent material constitutive behaviour, and thus the Ramberg–Osgood equations of sections I and II of the stress–strain curve of the material (cf. Table 2) may be expressed in terms of σ_{eq} and ε_{eq} (instead of σ and ε).

The crack was modelled as a round-tip slit with initial height (twice the tip radius) of 5 μm in agreement with experimental data for fatigue cracks in high-strength steels [19]. The simulated loading histories consisted of several (up to ten) zero-to-tension cycles in accordance with the majority of the experimental fatigue programmes, namely, at K_{max}/K_{IC} = 0.45, 0.60 and 0.80, followed by rising load corresponding to the HAC testing, as sketched in Fig. 4. The non-linear finite element code MARC [20] was used with updated lagrangian formulation.

The first point to be examined is the plasticity expansion during fatigue precracking, discriminating

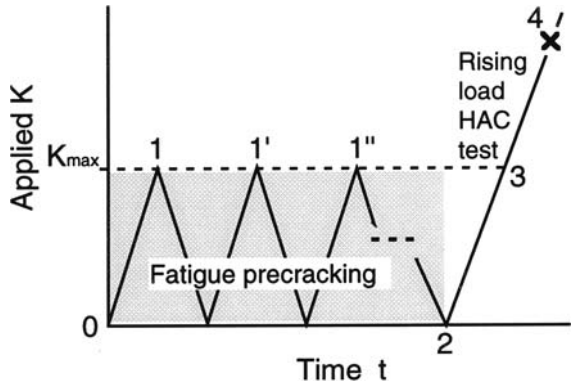

Fig. 4 Scheme of the experimental and simulated loading histories: shaded area (including points 0, 1, 1′, 1″ and 2) represents fatigue precracking, point 3 corresponds to monotonic loading during rising load HAC tests and point 4 (marked with cross) indicates the instant of hydrogen-assisted fracture at load F_{HAC}

between two crack tip plastic zones of interest. The first one is the commonly called *forward* or *monotonic* plastic zone, defined as the material region experiencing plastic deformation at cyclic load *maxima* $K = K_{max}$. The other smaller one, called the *reversed* or *cyclic* plastic zone, is the material domain where plasticity takes place at load *minima* $K = K_{min}$ (in the present study $K_{min} = 0$). Computational results show no appreciable dependence of these zones on the number of load cycles. In particular, the forward plastic zone is the same for the first attainment of the K_{max} level and the subsequent ones (points 1, 1′, 1″,..., 3 in Fig. 4), and therefore it is the same as the plastic zone for monotonic loading up to a specified K-level. Thus the dual nomenclature (forward or monotonic plastic zones) is seen to be adequate.

Performed numerical simulations in the matter of the plastic zones in the Von Mises sense, i.e., the domains where the equivalent Mises stress σ_{eq} exceeds the initial tensile yield stress σ_y (*stress-defined* plastic zone) are shown in Fig. 5. Indeed, within a particular fatigue regime (i.e., at a certain fixed K_{max} level) these respective forward and reversed zones are nearly invariable with the load cycle number. Comparing precracking histories with different K_{max}, the shapes of these zones look fairly self-similar with a scaling factor of $(K_{max}/\sigma_Y)^2$, common to a variety of fracture mechanics considerations.

The finite element analysis provides the following estimation of the depth of the forward plastic zone in the Von Mises sense (cf. Fig. 5a) measured in the same direction as the TTS depth in the experiments, i.e., ahead of the crack tip along the crack plane which coincides with the x-axis of the Cartesian coordinate system attached to the crack tip:

$$x_Y(K) = 0.0335\left(\frac{K}{\sigma_Y}\right)^2 \tag{1}$$

where impartial notation for the stress intensity factor K is used because the cyclic stability and self-similarity of these zones at all the top points $K = K_{max}$ of the loading paths imply that formula (1) is equally valid for the entire monotonic portions of loading patterns (paths 0–1 and 3–4 in Fig. 4) as well as at forward load maxima during cycling (points 1, 1′, 1″,... in Fig. 4). In particular, with $K = K_{max}$ formula (1) characterises the forward plastic domains during fatigue: $x_Y\ (K_{max}) = 0.0335\ (K_{max}/\sigma_Y)^2$. Conversely, the reversed plastic zone (computed at load minima using the von Mises criterion of yielding) is given in Fig. 5b, and the numerical results indicate that the extension $\Delta x_Y\ (K_{max})$ of this zone is about 0.2 times the respective forward zone size $x_Y(K_{max})$, i.e., $\Delta x_Y(K_{max}) \cong 0.2x_Y(K_{max}) \cong 0.007(K_{max}/\sigma_Y)^2$.

Going ahead with the evaluation of the plasticity expansion for strain-hardening materials, the criterion $\sigma_{eq} \geq \sigma_Y$ to define plastic zone using the initial tensile yield stress σ_Y (stress-defined plastic zone) is evidently applicable to describe the spreading of plasticity at the monotonic (first forward) loading and to mark the domain where plasticity has ever occurred, but not where it further proceeds at load reversals. This is because material strain-hardening modifies the stress

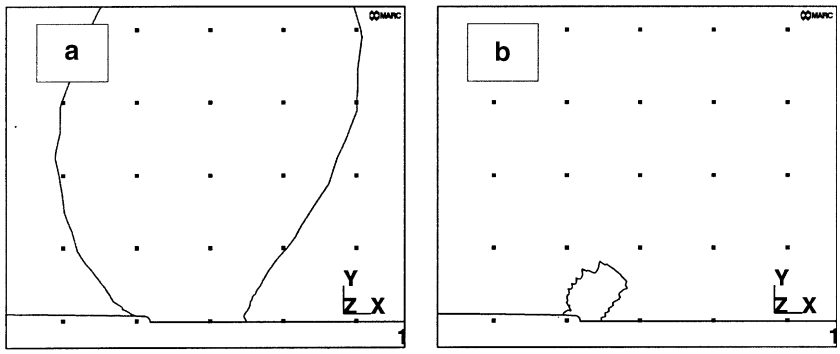

Fig. 5 *Von Mises* plastic zone (region in which $\sigma_{eq} \geq \sigma_Y$, i.e., *stress-defined* plastic zone) under cyclic loading at $K_{max}/K_{IC} = 0.80$: (**a**) *forward* or *monotonic plastic* zone at K_{max}; (**b**) *reversed* or *cyclic* plastic zone at K_{min}; both figures are in the same scale, and grid spacing is $0.015(K_{max}/\sigma_Y)^2 = 0.050$ mm

for yielding re-initiation at load reversals. These ''updated'' flow stresses are difficult to evaluate for complicated non-proportional stress–strain evolution patterns near the crack tip. Then, for non-monotonic loading paths, it is natural to define the *active plastic flow zones* from the condition of positive equivalent plastic strain rate $(d\varepsilon_{eq}^{p}/dt > 0)$ which indeed indicates where the active yielding (i.e., the dislocation movement) proceeds at arbitrary loading history. In contrast, the capability of stress-defined zones $\sigma_{eq} \geq \sigma_Y$ to represent the domains where plasticity really is going on seems to be inacceptable in this case.

Following the above reasoning, and to account for the role of cyclic plasticity produced during fatigue precracking, the *active*, really cyclic, plastic flow zones were obtained from the performed finite element solutions according to the criterion of positive plastic strain rate $(d\varepsilon_{eq}^{p}/dt > 0)$ which gives the domain associated with dislocation movement. An original and unexpected numerical result was obtained: these truly cyclic domains of active plastic straining (forward at K_{max} and reversed at K_{min} were seen to be again approximately cyclically stable, i.e. independent of the cycle number during constant amplitude fatigue in spite of hardening. Also, they appear to be self-similar with a scaling factor of $(K_{max}/\sigma_Y)^2$. This may be attributed to the diminishing hardening rate $d\sigma_{eq}/d\varepsilon_{eq}^{p}$ along the power-law strain-hardening curve at large strains. Figure 6 shows the size and shape of the active plastic zones at specific sequential instants of the loading process (fatigue precracking and rising-load HAC test, cf. Fig. 4), where it is seen that the reversed active yielding regions (at K_{min}) are similar to the forward active zones (at K_{max}), cf. Fig. 6a and c. As a first-order approximation, the depth of the forward active plastic zone at cyclic top loads (points 1′, 1″,..., 3 in Fig. 4) may be estimated as follows:

$$x_{\Delta}(K_{max}) = 0.0065\left(\frac{K_{max}}{\sigma_Y}\right)^2 \tag{2}$$

Figure 7 plots the evolutions of the depths of the active plastic zones through the whole rising-load HAC process for two different fatigue precracking regimes with $K_{max}/K_{IC} = 0.45$ and 0.80. The joint analysis of Figs. 6 and 7 allows a correct understanding of plasticity evolution during the test, as explained in the

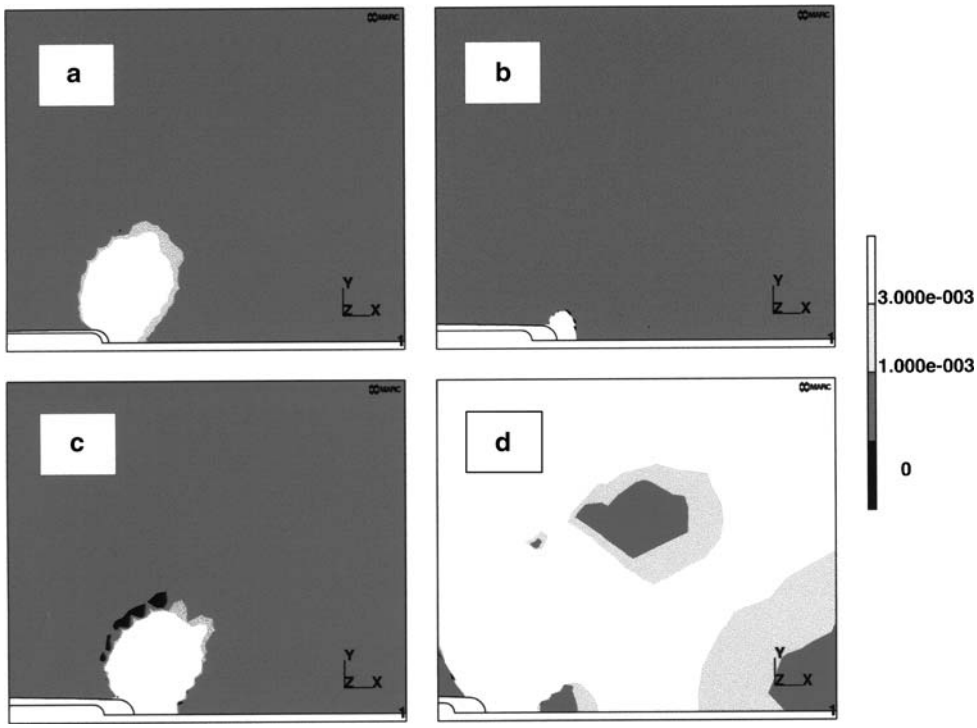

Fig. 6 *Active* plastic zone (region in which $d\varepsilon_{eq}^{p}/dt > 0$, i.e., *incremental or strain-defined* plastic zone where dislocation movement proceeds) during fatigue precracking at $K_{max}/K_{IC} = 0.80$ and subsequent rising load HAC test: (**a**) at load minima K_{min} during fatigue (point 2 in Fig. 4; *reversed* zone); (**b**) just after re-initiation of plastic flow after load reversal on the rising phase below K_{max} (between points 2 and 3 in Fig. 4); (**c**) at K_{max} (point 3, as well as points 1, 1′, 1″ in Fig. 4; *forward* zone); (**d**) active plastic zone burst just after exceeding K_{max}. All figures are in the same scale (equal to that in Fig. 5). The initial (radius 2.5 μm) and deformed crack tip shapes are in the bottom left corners. Plastic strain rates are shown in gray scale (right)

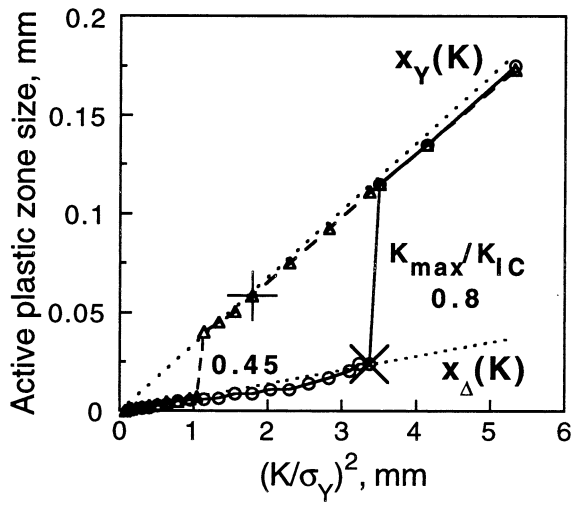

Fig. 7 Evolutions of the depths of active plastic zones in fatigue precracked specimens during rising load HAC tests: dashed and solid lines correspond respectively to fatigue regimes with $K_{max}/K_{IC} = 0.45$ and 0.80, crosses mark the instants of hydrogen-assisted fracture in experiments at respective levels of $K = K_{QHAC}$. Points represent the results of the finite element calculations and dotted lines show their approximations by the equations $x_Y(K) = 0.0335(K/\sigma_Y)^2$ and $x_\Delta(K) = 0.0065(K/\sigma_Y)^2$, respectively

following paragraphs devoted to sequential phases of the mechanical evolution in the close vicinity of the crack tip.

(i) *Initial phase.* At the beginning of the HAC test loading applied after precracking, increasing load causes stresses that, by superposition with the residual stress field after the final load reversal (unloading) in fatigue, result in elastic loading near the crack tip. Therefore, no plasticity occurs at this phase that lasts up to a certain applied stress intensity factor level slightly dependent on K_{max}. Corresponding average value of the stress intensity factor for initiation of plastic straining in the rising load HAC test for the considered range of K_{max} values may be estimated as $0.2K_{max}$. This value corresponds to the plastic zone in Fig. 6b, just after re-initiation of plastic flow after load reversal.

(ii) *Intermediate phase.* During further load increase in the HAC test, crack tip stress–strain fields evidently evolve the same way as during previous fatigue load whilst $K \le K_{max}$, i.e., plasticity development is identical to that observed on the forward portions of load cycles during precracking. So, active plastic deformations detected by the condition $d\varepsilon^p_{eq}/dt>0$ are confined to the cyclic plastic zones as described before (Fig. 6c and path $x_\Delta(K)$ in Fig. 7). Neglecting a short interval at the beginning of this phase where for obvious reasons the plastic zone must not be K-controlled and self-similar, relation (2) with K_{max} substituted by applied K turns out to be a good approximation for the plastic zone depth on this stage. Thus the forward active plastic zone size in this intermediate phase is $x_\Delta(K) = 0.0065(K/\sigma_Y)^2$. The maximum depth attained by the active plasticity in this phase is achieved at $K = K_{max}$ with a value $x_\Delta(K_{max})$.

(iii) *Final phase.* When applied load renders $K > K_{max}$ the equivalence of the stress-defined domain $\sigma_{eq} \ge \sigma_Y$ and the zone of increasing (active) plastic deformation $d\varepsilon^p_{eq}/dt > 0$ is restored since plasticity extends over new portions of material which has not experienced plastic deformation and yields when the initial flow stress σ_Y is attained, so that both of them define the same plastic region. The latter during this stage of the rising load test coincides with the monotonic plastic zone. Then formula (1) becomes valid again to represent the plastic zone depth. Therefore, when the K value applied during the HAC test exceeds the fatigue precracking level K_{max} the active plastic zone increases in a step-wise manner (''explodes'') in this loading stage (Fig. 6d and path $x_Y(K)$ in Fig. 7).

As a summary, the evolution of the active plastic zone where dislocation motion goes on during te rising load HAC test after fatigue precracking may be described as follows:

$$x_\perp(K) = \begin{cases} 0 & \text{at} \quad K \le 0.2K_{max} \\ x_\Delta(K) = 0.19x_Y(K) = 0.0065\left(\frac{K}{\sigma_Y}\right)^2 & \text{at} \quad 0.2K_{max} < K \le K_{max} \\ x_Y(K) = 0.0335\left(\frac{K}{\sigma_Y}\right)^2 & \text{at} \quad K > K_{max} \end{cases} \tag{3}$$

where the active plastic zone is represented now by the symbol $\perp$ to indicate the material region associated with dislocation movement. For low values of the externally applied K after precracking with a certain K_{max}, i.e., at the beginning of the HAC test ($K \leq 0.2K_{max}$), the active plastic zone is null, Later on ($K \leq 0.2K_{max} < K$), the depth of such a zone is given by $x_{\Delta}(K)$, i.e., it is the incremental or strain-defined plastic zone. Finally, when the level of externally applied K exceeds that of the last stage of fatigue precracking K_{max} ($K > K_{max}$) the depth of the active plastic zone is given by $x_Y(K)$, i.e., it is the Von Mises or stress-defined plastic zone. Described behaviour of the active plastic zone and of the dislocation movement region during the rising load HAC tests affected by fatigue precracking (Figs. 6, 7) provides the required tool for further analysis of the hydrogen–plasticity interactions.

Discussion

To analyse the results of the performed HAC tests on the basis of the described simulation of the crack tip mechanics, it is useful to compare in each experiment the two characteristic distances: (i) the computed depth of the active plastic zone $x_{\perp}$and (ii) the measured extension of the hydrogen-assisted damage area ahead of the crack tip (the TTS depth), both at the point of hydrogen-assisted fracture of the specimen. To define the former distance, the critical value of the stress intensity factor for HAC, K_{QHAC}, is evaluated from the ratio of the fracture load in hydrogen F_{HAC} to the same in air F_C (Fig. 1) as follows:

$$K_{QHAC} = \frac{F_{HAC}}{F_C} K_{IC}(\text{air}) \tag{4}$$

Neglecting subcritical crack growth, K_{QHAC} may be considered as an upper bound estimate for the threshold stress intensity factor for HAC.

The definition of K_{QHAC} allows a complete analysis of Fig. 7, where the yielding history is represented for HAC tests after precracking with $K_{max}/K_{IC} = 0.45$ and 0.80. As indicated above, there is a change in the plastic zone from strain-defined (incremental, i.e., associated with active plasticity) to stress-defined (von Mises) and this fact produces a kind of sudden increase (an ''explosion'') of plastic zone size. This sudden increase takes place when the maximum fatigue precracking level is exceeded during the rising-load HAC test, and thus it happens earlier in the lower precracking regimes ($K_{max}/K_{IC} = 0.45$) than in the heavier precracking regimes ($K_{max}/K_{IC} = 0.80$), as represented by the vertical lines in Fig. 7 (dashed $K_{max}/K_{IC} = 0.45$) and solid for $K_{max}/K_{IC} = 0.80$).

For each experimental fatigue precracking regime, Fig. 8 summarises the computational results in the matter of plasticity spreading. It presents the computed plastic zone sizes during fatigue precracking (forward or monotonic x_Y at the level $K = K_{max}$ and reversed or cyclic x_{Δ} at the level $K = K_{min} \cong 0$, for a given fatigue precracking intensity K_{max}). The active plastic zone depths $x_{\perp}$ at fracture in the rising load HAC test are also presented in Fig. 8. These latter regions are defined for corresponding experimental value of $K = K_{QHAC}$ according to the numerical results given by relations (3) and represent the physical domain where dislocation motion *does* take place in the material up to the fracture instant in the HAC test. For the lowest precracking level $K_{max} = 0.28K_{IC}$, the dimensions of interest in Fig. 8 were obtained by extrapolation of the numerical simulation data using relations (3), i.e., supposing a $(K/\sigma_Y)^2$-similitude of the near tip domain.

For lower precracking K_{max}-levels, the corresponding critical values are $K_{QHAC} > K_{max}$, and the active plastic zone at fracture $x_{\perp}(K_{QHAC})$ corresponds to the monotonic one $x_Y(K_{QHAC})$, whereas for the strongest fatigue precracking regime at $K_{max} = 0.80K_{IC}$ the

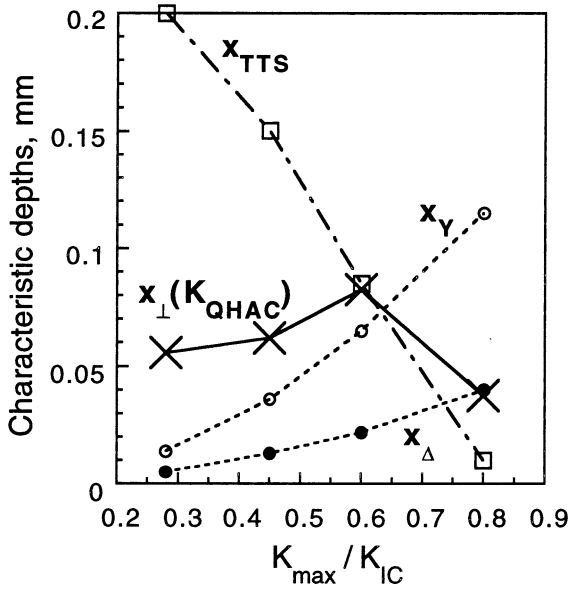

Fig. 8 Comparison of the scales of plasticity spreading and the sizes of the hydrogen-assisted microdamage region (TTS zone) near the crack tip depending on the fatigue precracking regime: dashed lines (with circles) show the sizes of the active cyclic and monotonic plastic zones $x_{\Delta}(K_{max})$ and $x_Y(K_{max})$, dashed-doted line (with squares) represents the measured TTS depth x_{TTS}, and the solid line (with crosses) marks the depth of active plasticity and dislocation movement at the instant of hydrogen-assisted fracture in the tests ($K = K_{QHAC}$)

critical value K_{QHAC} does not exceed K_{max} and the advancement of plastic straining is confined to the smaller cyclic plastic zone, $x_{\perp}(K_{QHAC}) = x_{\Delta}(K_{QHAC})$, cf. respective fracture points shown in Fig. 7. Just when the applied K level in a HAC test exceeds the fatigue precracking level ($K > K_{max}$), the active plastic zone changes from strain- to stress-defined, i.e., from cyclic to monotonic (or from reversed to forward), and this change produces a sudden increase of plastic zone size (an ''explosion'') the active plastic plastic zone $x_{\perp}$ where plastic flow goes on, i.e., $d\varepsilon_{eq}^{p}/dt > 0$.

To analyse the coupling between plasticity and hydrogenous effects, Fig. 8 offers the comparison of the calculated extensions $x_{\perp}$ of the active plastic flow (the scales of dislocations mobility) up to the hydrogen-assisted fracture event at $K = K_{QHAC}$ and the measured depths x_{TTS} of the hydrogen-assisted microdamage region (TTS) obtained after the HAC tests. With regard to the most forceful fatigue precracking programme with $K_{max} = 0.80K_{IC}$, this K_{max}-level is not surpassed during the HAC experiment because the test terminates just at that level, $K_{QHAC} \approx K_{max}$. Obviously, due to measurement errors this latter experimental value of K_{QHAC} may differ from K_{max} within some scatter band. Nevertheless, even if HAC really takes place at K_{QHAC} slightly higher than K_{max}, and so the active plastic zone may have the ''burst'' size at fracture, x_Y (K_{QHAC}) but not $x_{\Delta}(K_{QHAC})$ according to expression (3), it must not seriously affect the subsequent deductions from the comparisons of the $x_{\perp}(K_{QHAC})$ and the TTS depth x_{TTS} as far as during the main part of this test the plastic flow is confined to its reduced cyclic dimensions $x_{\Delta}(K)$ out of which insignificant plastic straining can proceed after exceeding K_{max} till soon test termination by HAC.

Figure 8 demonstrates that the development of the plastic zone where dislocation movement goes on does not seem to be a key item in the HAC process, due to the two fundamental experimental facts:

(i) In most experimental fatigue programmes (those with $K_{max}/K_{IC} = 0.28$, 0.45 and 0.60), the TTS depth is greater than the active plastic zone size associated with the movement of dislocations in the vicinity of the fatigue precrack tip during the HAC test.
(ii) The trends of evolution of the TTS and of the plastic zone sizes with the level of fatigue preloading K_{max}/K_{IC} are opposite. Whereas the size of the hydrogen-assisted microdamage region decreases with K_{max}, the plastic zone dimension increases with it.

On the basis of (i), it is possible to say that, in the majority of cases, the hydrogen-affected region exceeds the plastic zone, i.e., the only region in which there is dislocation movement, so that hydrogen transport cannot be attributed to dislocation dragging, but only to a random-walk diffusion. It is not, however, conventional diffusion according to classical Fick's laws, but stress-assisted diffusion in which the hydrostatic stress field plays a very important role in accelerating or delaying the diffusion depending on the sign of its gradient (cf. [3, 21]).

The proposed mechanism of transport by stress-assisted diffusion is consistent with the fundamental experimental fact shown in Fig. 1 of improved HAC behaviour for stronger fatigue precracking regimes. The higher the cyclic load level, the larger the plastic zone and the higher the compressive residual stresses generated near the crack tip after unloading. These compressive stresses are generated by strain compatibility in the plastic near-tip area surrounded by an elastic domain which compresses the former and they produce also negative hydrostatic stress in the vicinity of the crack tip, thus delaying the hydrogen entry and diffusion.

According to (ii) the TTS has no relationship with the plastic zone, and the opposite trends which exhibit these two magnitudes seem to indicate that the role of dislocations in hydrogen transport is reduced by enhancing the trapping of hydrogen instead of transporting it over long penetration distances. This is consistent with experimental observations of the effects of plastic deformation on hydrogen transport in iron, nickel and stainless steel [22] which did not support the assumption that moving dislocations accelerate hydrogen transport because of the two competing effects of enhanced transport and enhanced trapping.

The assumption of increasing trapping of hydrogen as a consequence of fatigue pecracking is consistent with an elevated predamage in the plastic zone created by fatigue within the cyclic plastic zone Δx_{PZ} which delays the hydrogen entry and diffusion transport by an increase of the dislocation density and thus of the number of potential traps for hydrogen, because such a density is known to be an increasing function of the accumulated plastic strain [23] and the latter is itself an increasing function of K_{max} as demonstrated in a previous work [24]. Thus the experimental fact of better HAC performance for increased K_{max} levels (Fig. 1) can also be explained by this phenomenon of trapping. The higher the K_{max}-level, the higher the density of traps and the lower the hydrogen diffusivity.

Moreover, an unambiguous support in favour of the insignificance of hydrogen transport by dislocations in

the considered HAC processes is provided by the last set of data in Fig. 8, i.e., those related to the strongest precracking regime at $K_{max}/K_{IC} = 0.8$. Indeed, the hydrogen-affected zone, as revealed by the TTS size, is much less than the dimension of any plastic zone there, either active cyclic one or the monotonic one on the phase of rising load HAC test. That is, hydrogen-assisted local (microscopic) fracture events occur at depths from the crack tip *much* shorter than the spreading of dislocation movement which supposedly could drag hydrogen towards local rupture sites, so that hydrogen accumulation in the fracture process zone cannot be attributed to its transport by dislocations. In contrast, short depth of the hydrogen-affected zone in this case correlates better with distance towards locations of the maximal hydrostatic stress beyond the crack tip, which is substantially less than the sizes of plastic zones according to [21].

A final reflection should be stated here. In the aforementioned cases in which the TTS zone is larger than the plastic zone (the big majority of tests), the final fracture process is not elastic, but elastic-plastic. The plastic zone analysed in this paper really means *primary plastic zone*, i.e., that obtained by elastic-plastic FEM analysis *without* introducing the crack extension generated by the TTS microfracture mode. The computation of this primary plastic zone is a first-order analysis under *fatigue precrack plasticity control.* As a matter of fact, there is a secondary plastic zone generated in the vicinity of the final crack tip (the TTS zone being considered as an extra-crack prolonging the original fatigue precrack), so that final fracture by cleavage is initiated in this secondary plastic zone under *final crack plasticity control.* However, the influence of this secondary plastic zone may be assumed to be negligible on hydrogen transport by dislocations to potential fracture places, since it appears after the development of the TTS crack. With the exception of the shortest tests, this happens at the final stages of loading (within the final 10%), considering the TTS depth at the end of the experiments and the crack growth rate associated with this topography [16, 18]. Thus a complicated second-order analysis (including progressive crack extension by TTS) does not seem to be necessary to obtain reliable conclusions on the interactions between hydrogen and plasticity in this pearlitic steel at the microscale.

Conclusions

It is shown that cyclic crack-tip plasticity improves the posterior HAC behaviour of the steel under monotonic loading, since the failure load in hydrogen is an increasing function of the maximum stress intensity factor during the last stage of fatigue precracking.

Fractographic analysis showed that the microdamage produced by hydrogen was clearly detectable by scanning electron microscopy through a specific microscopic topography associated with hydrogen effects: the *tearing topography surface* or *TTS*.

High-resolution numerical modelling demonstrated that both the monotonic and the cyclic plastic zone sizes in the fatigue precracking period stabilise after a few cycles and remain almost constant during fatigue, in spite of the constitutive equation of the material that includes strain-hardening.

When cyclic (fatigue) loading is applied during precracking, the active plastic zone where dislocation movement proceeds changes from the *forward* or *monotonic* one *(stress-defined) at* the maximum load to the *reversed* or *cyclic* one *(strain-defined)* at the minimum load. When the applied level of loading exceeds the historical maximum, a sudden increase (''explosion'') of the active plastic zone takes place.

In the majority of cases, the hydrogen-affected region exceeds the plastic zone, i.e., the only region in which there is dislocation movement, so that hydrogen transport cannot be attributed to dislocation dragging, but only to a random-walk diffusion. It is stress-assisted diffusion, according to which hydrogen is driven by the hydrostatic stress gradient.

The beneficial effect of crack tip plastic straining over the HAC may be due to the delay of hydrogen entry caused by compressive residual (hydrostatic) stress after precracking and by enhanced trapping of hydrogen as a consequence of plastic straining, which increases the dislocation density in the vicinity of the crack tip.

Acknowledgements The authors wish to thank the financial support of their research at the University of Salamanca provided by the following institutions: Spanish Ministry for Scientific and Technological Research MCYT-FEDER (Grant MAT2002-01831), Junta de Castilla y León (JCYL; Grant SA078/04) and Spanish Foundation ''Memoria de D. Samuel Solórzano Barruso''. In addition, the authors wish to express their gratitude to EMESA TREFILERIA S.A. (La Coruña, Spain) for providing the steel used in the experimental programme.

References

1. Troiano AR (1960) Trans ASM 52:54
2. Van Leeuwen HP (1974) Engng Fracture Mech 6:141
3. Toribio J, Kharin V (1997) Fatigue Fract Engng Mater Struct 20:729
4. Tien JK, Thompson AW, Bernstein IM, Richards RJ (1976) Metall Trans 7A:821

5. Johnson HH, Hirth JP (1976) Metall Trans 7A:1543
6. Nair SV, Jensen RR, Tien JK (1983) Metall Trans 14A:385
7. Toribio J (1993) J Mater Sci 28:2289
8. Toribio J (1992) J Mater Sci Lett 11:1151
9. Toribio J (1996) Mater Sci Engng A219:180
10. Toribio J, Lancha AM (1992) J Mater Sci Lett 11:1085
11. Toribio J, Lancha AM (1995) J Mater Sci Lett 14:1204
12. Toribio J, Lancha AM (1996) J Mater Sci 31:6015
13. Parkins RN, Elices M, Sánchez-Gálvez V, Caballero L (1982) Corros Sci 22:379
14. Thompson AW, Chesnutt JC (1979) Metall Trans 10A:1193
15. Costa JE, Thompson AW (1982) Metall Trans 13A:1315
16. Toribio J, Lancha AM, Elices M (1991) Scripta Metall Mater 25:2239
17. Toribio J, Lancha AM, Elices M (1992) Metall Trans 23A:1573
18. Toribio J (1997) Metall Mater Trans 28A:191
19. Handerhan KJ, Garrison WM Jr (1992) Acta Metall Mater 40:1337
20. MARC User Information, Marc Analysis Research Corporation, Palo Alto, 1994
21. Toribio J, Kharin V (1998) J Mech Behav Mater 9:205
22. Zakroczymski T (1985) Corrosion 41:485
23. Kumnick AJ, Johnson HH (1980) Acta Metall 28:33
24. Toribio J, Kharin V (2001) Mater Sci Engng A319–A321:535